# On optimal LISA orbit design

Yaguang Yang[*]

January 24, 2025

### Abstract

The ESA/NASA joint LISA (laser interferometer space antenna) mission is designed to detect gravitational waves, which relies crucially on maintaining three-spacecraft constellation as close to an equilateral triangle with a designed distance as possible. Efforts have been made to achieve this goal by using various simplified models to make it easy to approximately solve the complex problem. In this paper, the problem is formulated as a nonlinear optimization problem using exact nonlinear Kepler's orbit equations. It is shown that the optimal solution based on the exact nonlinear Kepler's orbit equations gives a better solution than the previously obtained ones.

**keywords:** LISA; formation fly; optimal orbit design

## 1  Introduction

LISA is an ESA/NASA mission with the objective of sensing low-frequency gravitational waves. Two sets of interferometers are installed on each of the three spacecraft. Each spacecraft's orbit is on a heliocentric plane. The three spacecraft are the three vertices of a moving (approximate) equilateral triangle with time-dependent distance variations around a designed length [3]. This variation introduces Doppler shifts and breathing angles which affect the interferometers' measurement [6, 8]. It is desirable to minimize the variation to meet the constraints of the motion range of the Optical Assembly Tracking Mechanism and the bandwidth limitation of the LISA phasemeter. The design of the best orbits that minimizes the distance variations about a designed length between the three spacecraft is a difficult nonlinear dynamics problem, therefore, various approximations have been considered by previous authors so that simplified problems based on approximate models can be solved [1, 3, 5, 6, 8]. In [5], the author searched for a solution using all six Keplerian elements. In [6], the Clohessy–Wiltshire (a first-order) model [2] is used to reduce the deviation in distance between the three

---

[*]NASA, Goddard Space Flight Center, 8800 Greenbelt Rd, Greenbelt, 20771 MD
Email: yaguang.yang@nasa.gov

spacecraft. In [3], a first-order approximation model is used and shows that the three-spacecraft constellation flies in an approximate equilateral triangle formation (we will refer to this orbit as the DNKV orbit). In [8], a second-order approximation model is used, aimed at improving the solution of [3] (we will refer to this orbit as the NKDV orbit). The orbit obtained in [8] is used as the baseline[1] for the LISA project [7]. Among six Keplerian elements, only the eccentricity and the inclination affect the magnitude of the distance variation, we may consider only these two Keplerian parameters to simplify the problem without sacrificing any accuracy in finding the optimal solution. On the other hand, using the exact nonlinear Keplerian orbit equations rather than an approximated model and optimizing for two variables (the eccentricity and the inclination) rather than just one (the tilt angle) should give us an exact optimal solution. In this article, we provide such an optimal solution and compare it with previously obtained ones. For this reason, we make the same assumptions used in [1, 3, 5, 8] in the discussion that the Sun is the only gravitating body in the solar system.

## 2   Two important orbit designs

Let the barycentric frame with coordinates (X,Y,Z) be defined as follows: the ecliptic plane is the X–Y plane and a circular reference orbit on the plane with radius $R = 1$ AU is centered at the Sun. For an elliptical orbit with its true focus at the Sun (true focus is defined in [13]), let $a$ be the semi-major axis and $e$ be the eccentricity, and $E$ be the eccentric anomaly. Following the definition of [3], we choose $t = 0$ at the time when the spacecraft is at aphelion, which is above the $+X$ axis. This coordinate system is different from many books and this choice of initial condition results in a positive sign instead of a negative sign in several equations below. The geometry of the orbit is shown in Figure 1. According to [11, page 92], the following relations hold.

$$X = a(\cos(E) + e), \ \ Y = a\sqrt{1 - e^2}\sin(E). \tag{1}$$

Let $\mu$ be the heliocentric gravitational constant and $\Omega = \sqrt{\mu/a^3}$ be the mean motion, then Kepler's equation is given by [11, page 53]

$$E + e\sin(E) = \Omega t, \tag{2}$$

where $\Omega t$ is the mean anomaly of the Sun. Let the orbit of spacecraft 1 be obtained by rotating the elliptical orbit about the $-Y$ axis by $i$ degrees so that its highest point (maximum $Z$) at t = 0 is in the positive $X$ direction, i.e., at this point, $E = 0$, $X = a(1 + e)\cos(i)$, $Y = 0$, and $Z = a(1 + e)\sin(i)$. In general, the orbit is given by

$$X_1(E) = a(\cos(E) + e)\cos(i), \tag{3a}$$

$$Y_1(E) = a\sqrt{1 - e^2}\sin(E), \tag{3b}$$

---

[1]This solution can be used as an initial guess for optimizing a full numerical nonlinear model which includes multiple gravitating bodies in the solar system [7]. As for nonlinear optimization problem (which may have many local optimizers), a good initial guess is very important.
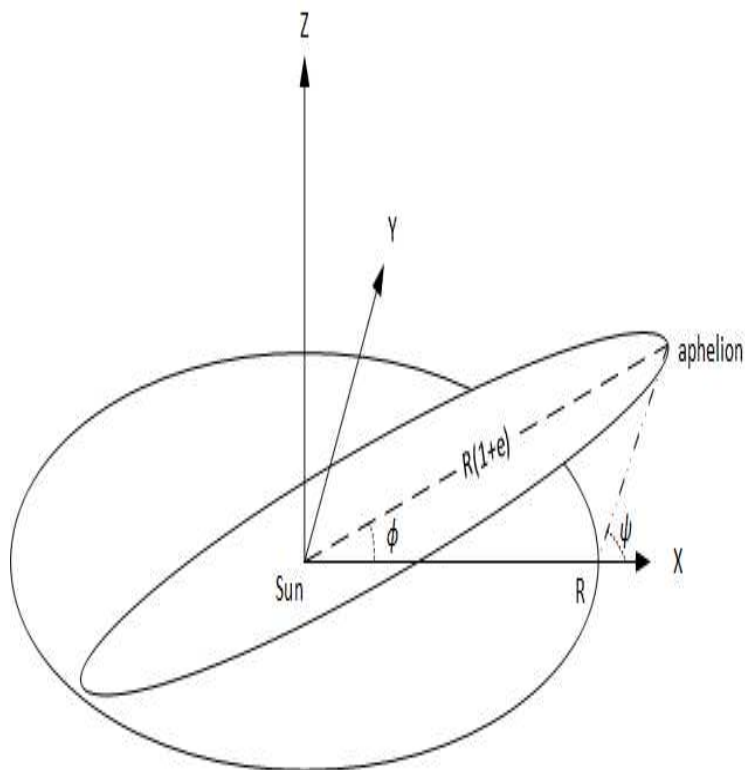
Figure 1: The geometry of the LISA spacecraft orbit with respect to the ecliptic plane.

$$Z_1(E) = a(\cos(E) + e)\sin(i) \tag{3c}$$

where $E$ is implicitly related to the time $t$ given by (2). Let the orbit of spacecraft 2 be obtained by rotating the orbit of spacecraft 1 about the $Z$ axis by $\frac{2}{3}\pi$ and the orbit of spacecraft 3 be obtained by rotating the orbit of spacecraft 1 about the $Z$ axis by $\frac{4}{3}\pi$. Then, their orbits can be represented by

$$X_k = X_1(E_k)\cos\left(\frac{2\pi}{3}(k-1)\right) - Y_1(E_k)\sin\left(\frac{2\pi}{3}(k-1)\right), \tag{4a}$$

$$Y_k = X_1(E_k)\sin\left(\frac{2\pi}{3}(k-1)\right) + Y_1(E_k)\cos\left(\frac{2\pi}{3}(k-1)\right), \tag{4b}$$

$$Z_k = Z_1(E_k), \tag{4c}$$

where $k = 1, 2, 3$, and $E_k$ implicitly depends on $t$ defined by Kepler's equations

$$E_k + e\sin(E_k) = \Omega t - (k-1)\frac{2\pi}{3}. \tag{5}$$

3

We will use this coordinate system throughout the paper. Let $\ell = 2,500,000$ km be the desired distance between any two spacecraft in the constellation, also denote $\alpha = \ell/2R$. In the rest of the paper, we will first review two existing orbit designs, then propose an optimal orbit design and compare their deviations from a desired distance.
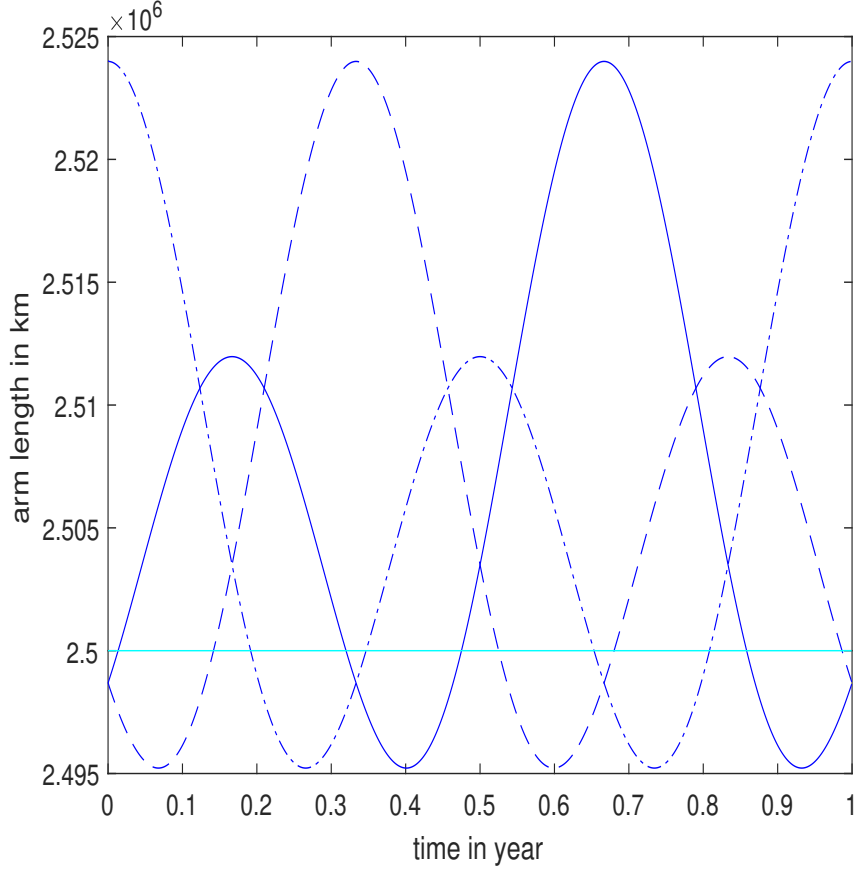
## 2.1 DNKV orbit



Figure 2: Spacecraft distances in one period of DNKV orbit. The horizontal line is the desired distance between any spacecraft pair. The solid line is the distance variation between spacecraft 1 & 2. The dashed line is the distance variation between spacecraft 1 & 3. The dashed-dot line is the distance variation between spacecraft 2 & 3.

In view of Figure 1, consider a line segment between the aphelion of spacecraft 1 and the intersection of the $X$ axis and the reference circular orbit on the ecliptic plan, the angle between the segment and the $X$ axis is denoted as $\psi$ and set $\psi = \pi/3$, Dhurandhar et al [3] have shown

$$\tan(i) = \frac{\alpha}{1 + \alpha/\sqrt{3}}, \quad e = \left(1 + \frac{2\alpha}{\sqrt{3}} + \frac{4\alpha^2}{3}\right)^{1/2} - 1, \tag{6}$$

4

and the constellation of spacecraft will fly almost like three vertices of a moving equilateral triangle (the distance between any two of the spacecraft is not strictly constant) with its center moving along the circular reference orbit. Given $\alpha$ and $a$, then, $e$ and $i$ can be calculated. Using (3), (4), and (5), the orbits of the three spacecraft can be obtained. The distances between any two of the three spacecraft are described in Figure 2, which is very similar to the one given in [3].

However, for the Laser Interferometer Space Antenna (LISA) constellation, it is desired to find an optimal solution such that the distances between any two of the spacecraft are as close to a desired constant as possible.
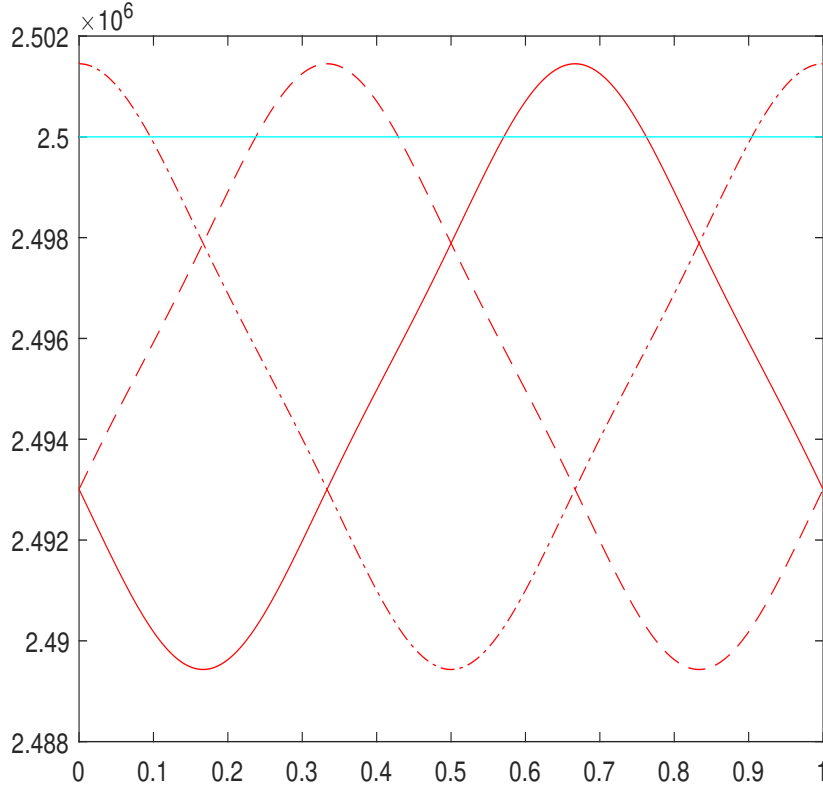
## 2.2 NKDV orbit



Figure 3: Spacecraft distances in one period of NKDV orbit. The horizontal line is the desired distance between any spacecraft pair. The solid lines are the distance variation between spacecraft 1 & 2. The dashed lines are the distance variation between spacecraft 1 & 3. The dashed-dot lines are the distance variation between spacecraft 2 & 3.

To reduce the distance variation, Nayak et al [8] allows the angle $\psi$ to be adjusted around $\pi/3$, i.e., $\psi = \pi/3 + \delta$. Using a second-order approximated model, they found

the best solution is $\delta = \frac{5}{8}\alpha$, and the following relations hold.

$$\tan(i) = \frac{2}{\sqrt{3}} \frac{\alpha \sin(\pi/3 + \delta)}{[1 + \frac{2}{\sqrt{3}}\alpha \cos(\pi/3 + \delta)]}, \qquad e = \left(1 + \frac{4\alpha^2}{3} + \frac{4\alpha}{\sqrt{3}}\cos(\pi/3 + \delta)\right)^{1/2} - 1. \quad (7)$$

Given $\alpha$, $\delta$, and $a$, then $e$ and $i$ can be calculated. Using (3), (4), and (5), the accurate orbits of the three spacecraft can be obtained. The distances between any two of the three spacecraft using accurate nonlinear model are presented in Figure 3. It is worthwhile to note that the accurate peak-to-peak distance using the nonlinear model for NKDV design is about 12,000 km which is a significant improvement over DNKV design (28,820 km). But the mean orbits of the three spacecraft are deviated from the designed $2.5 \times 10^6$ km, which is similar to the reported result in [7, Figure 3].

# 3   The optimal orbit design

The optimal orbit design is based on the arc-search techniques proposed in [15] for interior-point method.

## 3.1   An arc-search infeasible interior-point algorithm

Consider a general nonlinear optimization problem written as the following form:

$$\begin{aligned} \min \quad &: \quad f(\mathbf{x}) \\ \text{s.t.} \quad &: \quad \mathbf{h}(\mathbf{x}) = \mathbf{0}, \\ &\quad \mathbf{g}(\mathbf{x}) \geq \mathbf{0}, \end{aligned} \qquad (8)$$

where $f : \mathbb{R}^n \to \mathbb{R}$ is the nonlinear objective function, $\mathbf{h}(\mathbf{x}) = \mathbf{0}$ represents $m$ the nonlinear equalilty constraints, and $\mathbf{g}(\mathbf{x}) \geq \mathbf{0}$ represents $p$ the inequality constraints. The infeasible interior-point method has become popular to solve the nonlinear optimization problem [12]. The key idea of the method is to start with an initial point $\mathbf{x}^0$ that meets the nonlinear inequality constraints ($\mathbf{x}^0$ is an interior-point) but may NOT meet the equality constraints ($\mathbf{x}^0$ is an infeasible point) because it is very expensive to find a solution of the nonlinear system of equations $\mathbf{h}(\mathbf{x}) = \mathbf{0}$. However, as the iterate sequence $\{\mathbf{x}^k\}$ approximate the optimal solution $\mathbf{x}^*$, the iterates $\mathbf{x}^k$ will approach to a feasible solution (meeting both equality and inequality). The traditional optimization method uses linear search to find a better iterate in every iteration. This may not be a good strategy because the constraints are nonlinear. A benchmark test problem (HS-19) in Hock and Schittkowski [4] test set is used to justify why arc-search is a more appropriate search method.

$$\begin{aligned} \min \quad &: \quad f(\mathbf{x}) = (x_1 - 10)^3 + (x_2 - 20)^3 \\ \text{s.t.} \quad &: \quad (x_1 - 5)^2 + (x_2 - 5)^2 - 100, \geq 0 \\ &\quad -(x_2 - 5)^2 - (x_1 - 6)^2 + 82.81 \geq 0, \\ &\quad 13 \leq x_1 \leq 100, \\ &\quad 0 \leq x_2 \leq 100. \end{aligned} \qquad (9)$$

6

For this problem, the last 4 boundary inequalities are redundent. The area of the constraint is depicted in Figure 4, which is between two red curves. The contour lines represent the levels of the objective function, which decrease in the top-down direction. The optimal solution is at the interception of the two red curves marked with a red 'x'. Clearly, for an iterate inside the area of the constraint, searching along a decreasing line segment for optimizer is not as good as searching along an arc described in Figure 5 which is part of an ellipse.
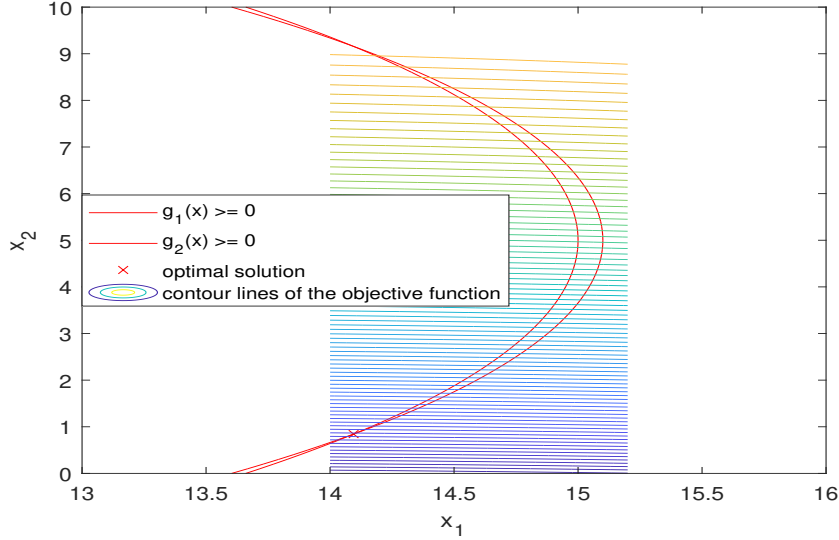


Figure 4: The constraint of HS-19.

For problem (9) depicted in Figure 5, the arc (represented in blue color) passing the current iterate (marked with a red 'o') can be obtained systematically and be used to search for the optimizer. The merit of using arc-search for the interior-point method can be seen from Figure 5 and was analyzed in an internal report [17, 16] where an efficient algorithms is proposed and the convergence is analyzed[2]. An optimization tool that implements the algorithm in [16] by the author and provides the ability to compute first and second order derivatives via an automatic differentiation[3] tool of [10] with improved the speed and accuracy was used to solve the optimal orbit design problem (11) to be discussed.

## 3.2 Optimal orbit design assuming identical $e_k$ and $i_k$ for all spacecraft $k$

Without loss of generality, we may assume each spacecraft's orbit is elliptic meaning its size and shape depend only on $a$ and $e$. Since the constellation's period should be the same as the Earth's period, this means that $a = R$. Each spacecraft orbit is inclined

---

[2]The algorithm is an improved version of the arc-search infeasible interior-point algorithm of [14]
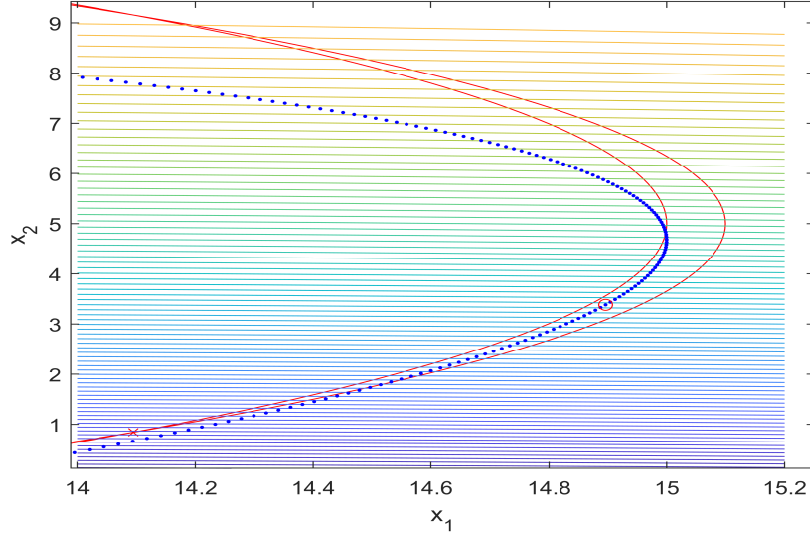[3]Details about automatic differentiation are discussed in [9, Section 7.2].

Figure 5: The arc used for searching optimizer at current iterate of Problem (9).

with respect to the ecliptic plan by an angle $i$. Therefore, only $e$ and $i$ are independent, and should be optimized ($\delta$ is implicitly determined by $i$ therefore is redundant). We formalize the orbit design problem as an optimization problem that directly selects the optimal $i$ and $e$ to minimize the distance deviation from a desired constant, while meeting all constraints defined by (3), (4), and (5).

Let $T = \frac{2\pi}{\Omega}$ be the period of the three spacecraft orbits. For $0 = t_0 < t_1 < \ldots < t_{n-1} < t_n = T$, the desired distance between spacecraft $i$ and $j$ (for $1 \leq i < j \leq 3$) is $\ell_{i,j} = 2,500,000$ km, and the distance deviation between spacecraft $i$ and $j$ at $t_k$ from the desired distance is given by

$$d_{i,j}(t_k) = \sqrt{(X_i(t_k) - X_j(t_k))^2 + (Y_i(t_k) - Y_j(t_k))^2 + (Z_i(t_k) - Z_j(t_k))^2} - \ell_{i,j}. \quad (10)$$

Our objective is to minimize the accumulative distance deviation (10) for all $t_k$, subject to satisfying the orbital requirements of (3), (4), and (5) for all $t_k$. In addition, we impose some safe boundary constraints on $e$ and $i$, aiming at accelerating the
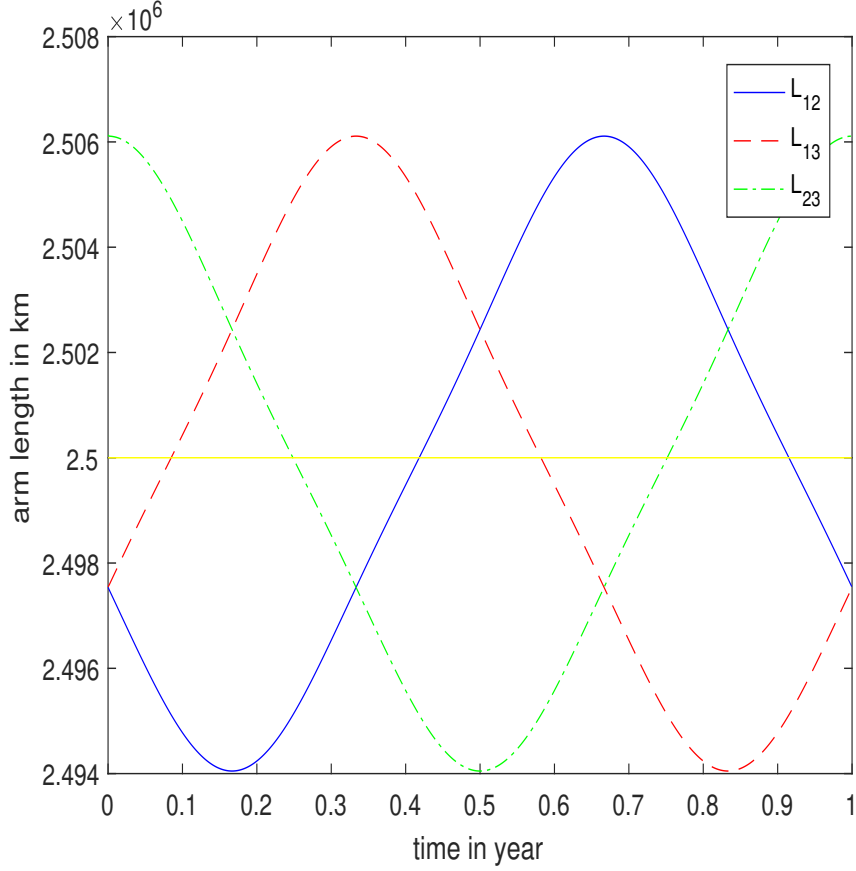
Figure 6: Spacecraft distances in one period of optimal orbit. The horizontal line is the desired distance between any spacecraft pair. The solid line is the distance variation between spacecraft 1 & 2. The dashed line is the distance variation between spacecraft 1 & 3. The dashed-dot line is the distance variation between spacecraft 2 & 3.

convergence rate. Therefore, the optimization problem can be written as follows.

$$
\begin{aligned}
\min \quad & \sum_{t_k=0,\ldots,T} \sum_{1 \le i < j \le 3} d_{i,j}^2(t_k) \\
\text{s.t.} \quad & E_1(t_k) + e\sin(E_1(t_k)) = \Omega t_k, \\
& E_2(t_k) + e\sin(E_2(t_k)) = \Omega t_k - \tfrac{2\pi}{3}, \\
& E_3(t_k) + e\sin(E_3(t_k)) = \Omega t_k - \tfrac{4\pi}{3}, \\
& X_1(E_1(t_k)) = a(\cos(E_1(t_k)) + e)\cos(i), \\
& Y_1(E_1(t_k)) = a\sqrt{1-e^2}\sin(E_1(t_k)), \\
& Z_1(E_1(t_k)) = a(\cos(E_1(t_k)) + e)\sin(i) \\
& X_2(t_k) = X_1(E_2(t_k))\cos\left(\tfrac{2\pi}{3}\right) - Y_1(E_2(t_k))\sin\left(\tfrac{2\pi}{3}\right), \\
& Y_2(t_k) = X_1(E_2(t_k))\sin\left(\tfrac{2\pi}{3}\right) + Y_1(E_2(t_k))\cos\left(\tfrac{2\pi}{3}\right), \\
& Z_2(t_k) = Z_1(E_2(t_k)), \\
& X_3(t_k) = X_1(E_3(t_k))\cos\left(\tfrac{4\pi}{3}\right) - Y_1(E_3(t_k))\sin\left(\tfrac{4\pi}{3}\right), \\
& Y_3(t_k) = X_1(E_3(t_k))\sin\left(\tfrac{4\pi}{3}\right) + Y_1(E_3(t_k))\cos\left(\tfrac{4\pi}{3}\right), \\
& Z_3(t_k) = Z_1(E_3(t_k)), \\
& 0 = \Omega t_0 < \Omega t_1 < \ldots < \Omega t_{n-1} < \Omega t_n = 2\pi, \\
& 0 \le e \le 0.01, \quad 0 \le i \le \pi/6,
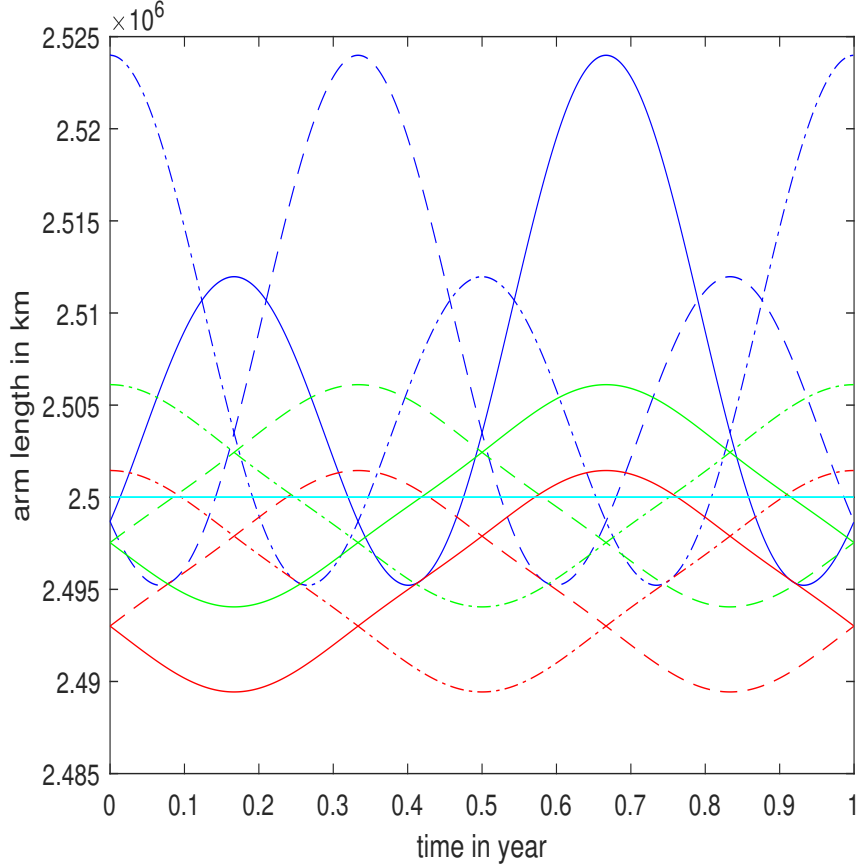\end{aligned}
\tag{11}
$$

9

Figure 7: Distances comparison of all three orbit designs. The capri line is the desired distance between any spacecraft pair. The blue lines are orbit distances between spacecraft pairs of DNKV orbit design. The red lines are orbit distances between spacecraft pairs of NKDV orbit design. The green lines are orbit distances between spacecraft pairs of the optimal orbit design. The solid lines are orbit distances between spacecraft 1 & 2. The dashed lines are orbit distances between spacecraft 1 & 3. The dashed dot lines are orbit distances between spacecraft 2 & 3.

where $i$ and $e$ are independent variables, and $0 \leq \Omega t_k \leq 2\pi$. For the fixed $i$ and $e$, it is clear that $E_1$, $E_2$, and $E_3$ are functions of $t_k$. In addtion, $X_i$, $Y_i$, and $Z_i$ are functions of $E_i(t)$, $i = 1, 2, 3$.

Starting from a feasible solution $(e, i) = (0.0047975, 0.008315)$ (which is determined based on some trial-and-error process), after 14 iterations, we find the optimal solution

$$(e^*, i^*) = (0.004824385965325, 0.008355663130457).$$

The distances between any two of the three spacecraft are obtained from (3), (4), and (5). The result is presented in Figure 6. The comparison of all three designs is presented in Figure 7. The distance change of DNKV design is about $2.8789e + 04$ kilometers, the distance change of NKDV design is about $1.2e + 04$ kilometers, which is essentially

10

the same one as the optimal design. But latter is centered about $2.5 \times 10^6$ km while the former is not.

## 3.3 Optimal orbit design assuming different $e_k$ and $i_k$ for all spacecraft $k$

In this design, we assume that the eccentricity and inclination of spacecraft $k$ are $e_k$ and $i_k$ for $k = 1, 2, 3$. We would like to know, under this assumption, if we can find a better optimal design using the extra degrees of freedom. For this purpose, Kepler's equation for the three spacecraft is given as follows.

$$E_k + e_k \sin(E_k) = \Omega t - (k-1)\frac{2\pi}{3}, \quad \text{for } k = 1, 2, 3. \tag{12}$$

Accordingly, the orbits of the three spacecraft at the same orientation are modified as

$$\tilde{X}_k(E_k) = a(\cos(E_k) + e_k)\cos(i_k), \text{for } k = 1, 2, 3, \tag{13a}$$

$$\tilde{Y}_k(E_k) = a\sqrt{1 - e_k^2}\sin(E_k), \quad \text{for } k = 1, 2, 3, \tag{13b}$$

$$\tilde{Z}_k(E_k) = a(\cos(E_k) + e_k)\sin(i_k), \text{for } k = 1, 2, 3. \tag{13c}$$

Finally, the desired orbits of the three spacecraft are given by

$$X_k = \tilde{X}_k(E_k)\cos\left(\frac{2\pi}{3}(k-1)\right) - \tilde{Y}_k(E_k)\sin\left(\frac{2\pi}{3}(k-1)\right), \quad \text{for } k = 1, 2, 3, \tag{14a}$$

$$Y_k = \tilde{X}_k(E_k)\sin\left(\frac{2\pi}{3}(k-1)\right) + \tilde{Y}_k(E_k)\cos\left(\frac{2\pi}{3}(k-1)\right), \quad \text{for } k = 1, 2, 3, \tag{14b}$$

$$Z_k = \tilde{Z}_k(E_k), \quad \text{for } k = 1, 2, 3. \tag{14c}$$

Combining all above formulas yields the optimization problem:

$$
\begin{aligned}
\min \quad & \sum_{t_k=0,\ldots,T} \sum_{1 \le i < j \le 3} d_{i,j}^2(t_k) \\
\text{s.t.} \quad & E_1(t_k) + e_1 \sin(E_1(t_k)) = \Omega t_k, \\
& E_2(t_k) + e_2 \sin(E_2(t_k)) = \Omega t_k - \frac{2\pi}{3}, \\
& E_3(t_k) + e_3 \sin(E_3(t_k)) = \Omega t_k - \frac{4\pi}{3}, \\
& X_1(E_1(t_k)) = a(\cos(E_1(t_k)) + e_1) \cos(i_1), \\
& Y_1(E_1(t_k)) = a\sqrt{1 - e_1^2} \sin(E_1(t_k)), \\
& Z_1(E_1(t_k)) = a(\cos(E_1(t_k)) + e_1) \sin(i_1) \\
& \tilde{X}_2(E_2(t_k)) = a(\cos(E_2(t_k)) + e_2) \cos(i_2), \\
& \tilde{Y}_2(E_2(t_k)) = a\sqrt{1 - e_2^2} \sin(E_2(t_k)), \\
& \tilde{Z}_2(E_2(t_k)) = a(\cos(E_2(t_k)) + e_2) \sin(i_2) \\
& \tilde{X}_3(E_3(t_k)) = a(\cos(E_3(t_k)) + e_3) \cos(i_3), \\
& \tilde{Y}_3(E_3(t_k)) = a\sqrt{1 - e_3^2} \sin(E_3(t_k)), \\
& \tilde{Z}_3(E_3(t_k)) = a(\cos(E_3(t_k)) + e_3) \sin(i_3) \\
& X_2 = \tilde{X}_2(E_2) \cos\left(\frac{2\pi}{3}\right) - \tilde{Y}_2(E_2) \sin\left(\frac{2\pi}{3}\right), \\
& Y_2 = \tilde{X}_2(E_2) \sin\left(\frac{2\pi}{3}\right) + \tilde{Y}_k(E_k) \cos\left(\frac{2\pi}{3}\right), \\
& Z_2 = \tilde{Z}_2(E_2), \\
& X_3 = \tilde{X}_3(E_3) \cos\left(\frac{4\pi}{3}\right) - \tilde{Y}_3(E_3) \sin\left(\frac{4\pi}{3}\right), \\
& Y_3 = \tilde{X}_3(E_3) \sin\left(\frac{4\pi}{3}\right) + \tilde{Y}_k(E_3) \cos\left(\frac{4\pi}{3}\right), \\
& Z_3 = \tilde{Z}_3(E_3), \\
& 0 = \Omega t_0 < \Omega t_1 < \ldots < \Omega t_{n-1} < \Omega t_n = 2\pi, \\
& 0 \le e \le 0.01, \quad 0 \le i \le \pi/6,
\end{aligned}
\tag{15}
$$

Starting from the following feasible point

$$(e_1, i_1, e_2, i_2, e_3, i_3,) = (0.0047975, 0.008315, 0.0047975, 0.008315, 0.0047975, 0.008315),$$

after 14 iteration, we obtain an optimal solution

$$(e_1, i_1, e_2, i_2, e_3, i_3,) = (0.0048244, 0.0083556, 0.0048243, 0.0083556, 0.0048243, 0.0083556),$$

which is essentially the same result we obtained in the previous section. Starting from some random initial points near the above optimal solution, we reached the same result. This means that the optimal solution of (11) is likely a global optimal solution of (15). Since problem (11) is simpler than problem (15), it is more efficient to solve (11) than solve (15).

## 3.4 Extension to $n$ spacecraft in formation fly

We have discussed the solution of 3 spacecraft in formation fly. The method discussed in Section 3.2 can easily be extended to the case of $n \ge 4$ spacecraft in formation fly. The key idea is to use (2) and (3) to represent the orbit of Spacecraft 1. Then the orbit presentation for the $k$-th $(k = 2, \ldots, n)$ spacecraft can be obtained by rotating the orbit of Spacecraft 1 by $360(k-1)/n$ degrees about the center of the coordinate system

(the Sun, see Figure 1). Following exactly the same procedure in Section 3.2, we can obtain an optimization problem similar to (11), and the optimization algorithm/tool developed in [16] can be used to solve the general problem.

# 4    Conclusions

The LISA orbit design problem is formulated as a nonlinear optimization problem using exact nonlinear Kepler's orbit equations. The problem is solved by using an arc-search interior-point algorithm. The solution minimizes the distance variations about a designed constant between the three LISA spacecraft, thereby reducing the Doppler shift and breathing angle effects on the measurement of gravitational waves.

# 5    Acknowledgements

# 6    Data availability statement

The matlab code that is used to generate the result is available upon reasonable request.

# References

[1] J. C. Amato, Flying in formation: The orbital dynamics of LISA's three spacecraft, Am. J. Phys. 87 (1), 18-23, 2019.

[2] W. Clohessy, and R. Wiltshire, Terminal guidance system for satellite rendezvous, Journal of Astronautical Sciences, 27(9), 653–678, 1960.

[3] S. V. Dhurandhar, K.R. Nayak, S. Koshti, and J-Y Vinet, Fundamentals of the LISA stable flight formation, Classical and Quantum Gravity, 22, 481–487, 2005.

[4] W. Hock and K. Schittkowski, Test examples for nonlinear programming codes, in Lecture Notes in Economics and Mathematical Systems, volume 187, Springer, 1981.

[5] S.P. Hughes, Preliminary optimal orbit design for laser interferometer space antenna, 25th Annual AAS Guidance and Control Conference (Breckenridge CO, Feb. 2002)

[6] F. De Marchi, G. Pucacco, and M Bassan, Optimizing the Earth–LISA 'rendezvous', Classical and Quantum Gravity, 29 (2012) 035009

[7] W. Martens and E. Joffre, Trajectory Design for the ESA LISA Mission, J Astronaut Sci 68, 402–443, 2021.

[8] K.R. Nayak, S. Koshti, S. V. Dhurandhar, and J-Y Vinet, On the minimum flexing of LISA's arms, Classical and Quantum Gravity, 23, 1763–1778, 2006.

[9] J. Nocedal and S. J. Wright, Numerical Optimization, Springer, New York, 2006.

[10] Siegfried M. Rump, INTLAB - INTerval LABoratory, https://www.tuhh.de/ti3/rump/intlab/, last accessed on 12/2/2023.

[11] D. A. Vallado, Fundamentals of astrodynamics and applications, Springer Science & Business Media; pp. 310-316, 2001 Jun 30.

[12] A. Wächter and L. T. Biegler, Line search filter methods for nonlinear programming: motivation and global convergence, SIAM Journal on Optimization 16(1), 1-31, 2005.

[13] B. Wie, Space Vehicle Dynamics and Control, AIAA Education Series, AIAA Inc., Reston, 1998.

[14] M. Yamashita, E. Iida, and Y. Yang An infeasible interior-point arc-search algorithm for nonlinear constrained optimization, Numerical Algorithms, 12, 781–798, 2018.

[15] Y. Yang, Arc-search techniques for interior-point methods, CRC Press, Baco Raton, 2020.

[16] Y. Yang, An arc-search interior-point algorithm for nonlinear constrained optimization, Computational Optimization and Applications, 2025, 10.1007/s10589-025-00648-1, published online https://rdcu.be/d57NX.

[17] Y. Yang, R. Pritchett, and N. Hatten, An infeasible interior-point arc-search algorithm for spacecraft trajectory optimization, INFORMS Optimization 2024, Huston, March 22-24, 2024. Available on https://ntrs.nasa.gov/citations/20240002037